Inorganic Chemistry

pubs.acs.org/IC Article

A Robust Cage-Based Metal−Organic Framework Showing Ultrahigh SO_2 Uptake for Efficient Removal of Trace SO_2 from SO_2/CO_2 and $SO_2/CO_2/N_2$ Mixtures

Meng Jia Yin, Xiao Hong Xiong, Xue Feng Feng, Wen Yuan Xu, Rajamani Krishna, and Feng Luo*

Cite This: *Inorg. Chem.* 2021, 60, 3447−3451 Read Online

ACCESS | Metrics & More | Article Recommendations | Supporting Information

ABSTRACT: Removal of trace SO_2 from an SO_2-containing product is now receiving increasing attention. However, designing a robust porous adsorbent with high SO_2 adsorption capacity and good SO_2/CO_2 selectivity, as well as validity under humid conditions, is still a challenging task. Herein, we report a porous cage-based metal−organic framework, namely ECUT-111, which contains two distinct cages with apertures of 5.4 and 10.2 Å, respectively, and shows high a BET of up to 1493 m^2/g and a pore volume of 0.629 cm^3/g. Impressively, ECUT-111 enables an ultrahigh SO_2 uptake of up to 11.56 mmol/g, exceeding most reported top-performing adsorbents for such a use. More importantly, complete separation of trace SO_2 from SO_2/CO_2 and $SO_2/CO_2/N_2$ mixtures, especially under humid conditions, and excellent recycle use were observed for ECUT-111, suggesting its superior application in desulfurization of SO_2-containing products.

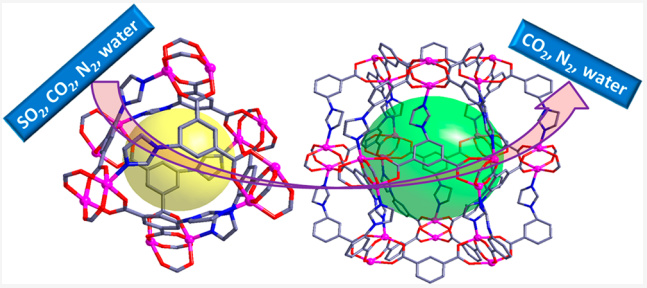

INTRODUCTION

Metal−organic frameworks are a newly developed porous platform. This category is in principle constructed by metal ions and organic ligands via coordination bonds.[1−3] Thanks to the proof of concept of reticular and topology chemistry, we can deliberately design and create target-desired MOFs for advanced host−guest recognition.[4,5] To rationally construct the desired MOFs, utilizing documented secondary building blocks (SBBs) such as paddlewheel units of Zn_2, Cu_2, and Co_2,[6] trigonal Cr_3O and Fe_3O units,[7] a tetrahedral Zn_4O unit,[8] 12-connecting Zr_6 or Th_6 units,[9] and rod-shaped units[10] or generating new SBBs[11] to enrich the database of SBBs are highly important. Among these SBBs, a cage-based SBB presents a unique species, as it contains inherent inner porosity and often has multiple pore features with different pore sizes. Especially, a cage not only has a narrow window, capable of providing a molecular sieve effect for selective host−guest recognition, but also affords a large inherent inner cavity, benefiting the enhancement of guest uptake and thus making these species especially good for separation applications.[12] For example, Zhang et al. reported a Th_4-cage-based MOF with high stability and interesting gas adsorption properties.[12b]

Sulfur dioxide (SO_2) resulting from volcanic eruptions, the combustion of coal and oil, and the use of SO_2-containing products is now viewed to be one of the major atmospheric pollutants. SO_2 has strong acidity and causticity and should not be directly released into the air, as this will seriously harm the environment and human health.[13] Trace SO_2 in a SO_2-containing product could also largely reduce its function or even lead to invalidation. To eliminate this contamination, the traditional method is wet flue gas desulfurization (FGD) technology; however, this inevitably causes the consumption of a great deal of energy and causes a large amount of waste.[14] To upgrade this technology, an adsorbent-based separation approach was proposed.[15] Although commercial activated carbon is effective, its low adsorption capacity and weak SO_2/CO_2 selectivity prevent its use for practical applications. For SO_2 removal, one major challenge is the trace amount of SO_2 at the ppm level, in contrast to the abundant counterpart of CO_2, which consequently requires a high selectivity of SO_2 over CO_2. The other major issue is the strong acidity and causticity of SO_2, which could destroy most MOFs during the SO_2 adsorption process, especially under humid conditions, thus largely reducing the separation performance or even leading to invalidation. Thereby, MOFs available for SO_2 removal, especially under humid conditions, are still highly scarce.[16]

In this work, we report a novel MOF, ECUT-111, which is composed of two distinct cages. A high porosity, as evidenced

Received: January 6, 2021
Published: February 17, 2021

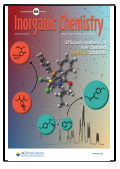

https://dx.doi.org/10.1021/acs.inorgchem.1c00033
Inorg. Chem. 2021, 60, 3447−3451

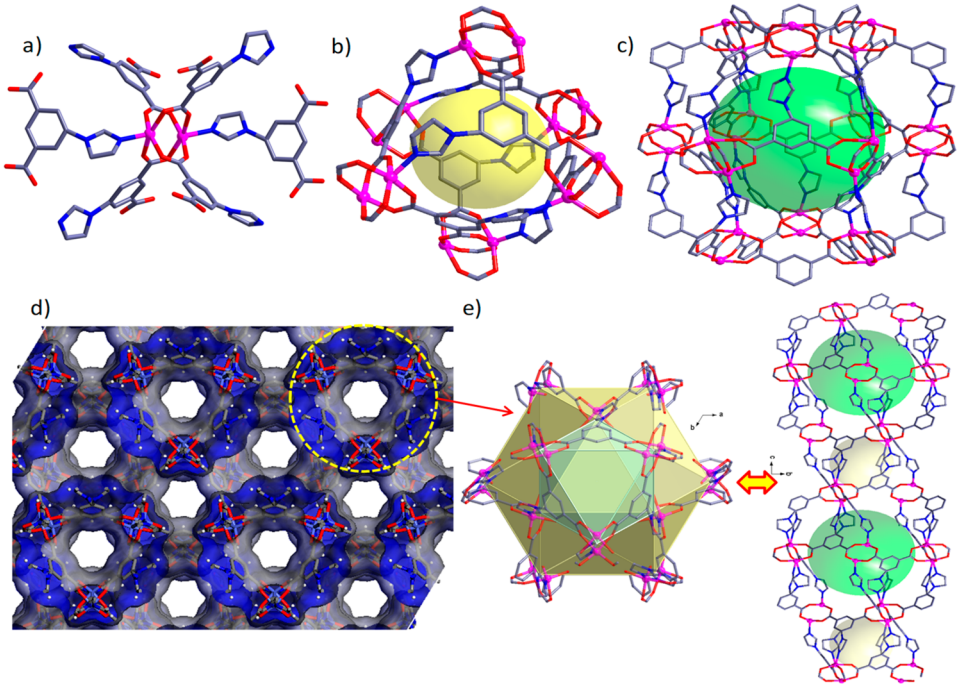

Figure 1. (a) View of the Co_2 paddlewheel unit connecting to six L^{2-} ligands. Color code: purple, Co; blue, N; red, O; gray, C. (b) View of cage A. (c) View of cage B. (d) View of the 3D cage-based framework. (e) View of the in-turn connected cages A and B.

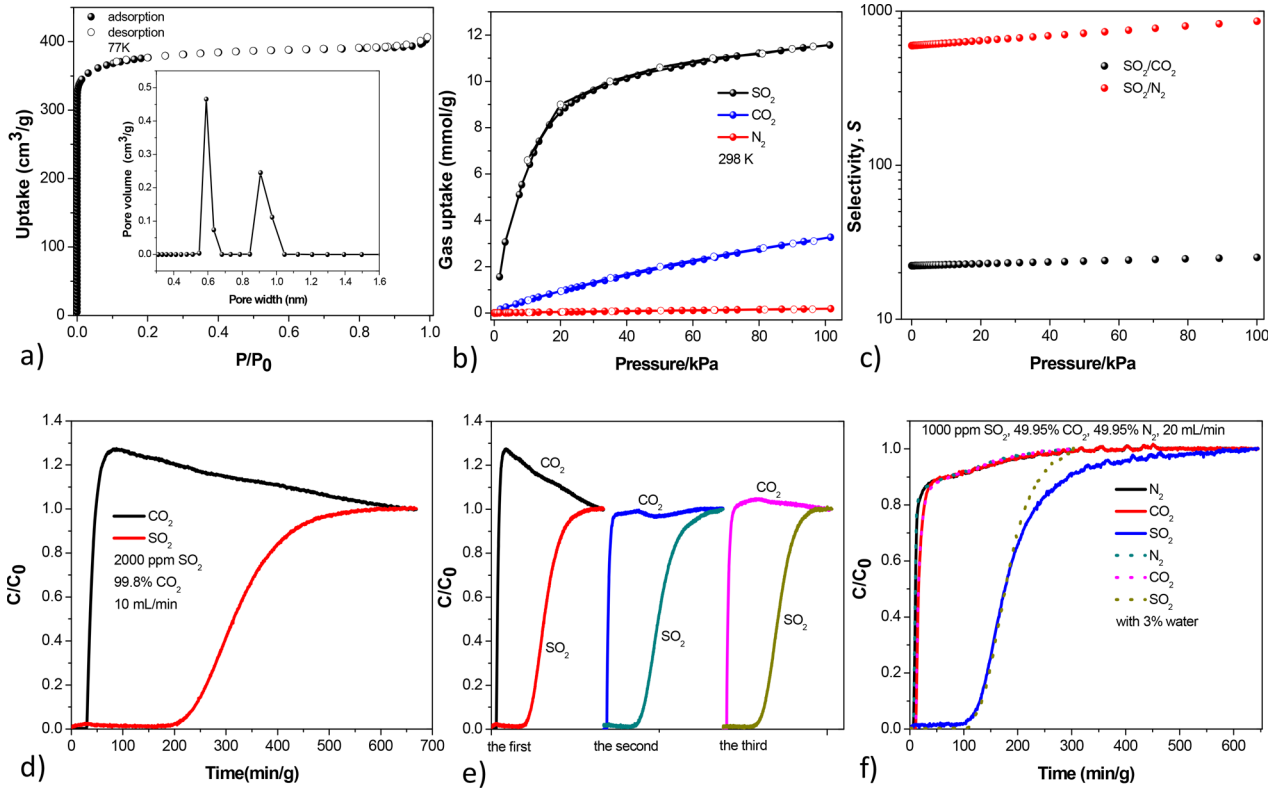

Figure 2. (a) N_2 adsorption isotherm at 77 K. The inset shows the pore distribution. (b) SO_2, CO_2, and N_2 adsorption and desorption isotherms at 298 K, where reversible desorption isotherms for SO_2, CO_2, and N_2 were observed. (c) SO_2/CO_2 and SO_2/N_2 selectivity for a 1/99 v/v SO_2/CO_2 or SO_2/N_2 mixture. (d) Breakthrough experiments upon an ECUT-111 bed (0.5 g) under a 10 mL/min flow for a SO_2/CO_2 mixture. (e) Recycling ability of ECUT-111 in separating a SO_2/CO_2 mixture. (f) Comparison of separating a $SO_2/CO_2/N_2$ mixture without water and with 3% water.

by high BET and pore volume, was observed for ECUT-111. This MOF enables an ultrahigh SO_2 adsorption capacity and SO_2/CO_2 selectivity. The real application of it for SO_2 removal was confirmed by experimental breakthrough tests.

RESULTS AND DISCUSSION

The MOF (ECUT-111, [Co(L)], H_2L= 5-(1*H*-imidazol-1-yl) isophthalic acid) was synthesized by self-assembly of H_2L with

https://dx.doi.org/10.1021/acs.inorgchem.1c00033
Inorg. Chem. 2021, 60, 3447−3451

$Co(NO_3)_2$ in a DMF (4 mL)/C_2H_5OH (1 mL) mixture with 200 μL of HNO_3 at 150 °C for 3 days. Pure red block crystals were obtained in a yield of up to 75% based on Co. The phase purity was confirmed by powder X-ray diffraction (PXRD, Figure S1).

The structure of ECUT-111 was determined by single-crystal X-ray diffraction, showing a rhombohedral crystal system and $R\bar{3}$ space group. One crystallographically independent Co site is observed, showing the common pyramidal geometry completed by four carboxylate oxygen atoms from four L^{2-} ligands and one imidazole nitrogen atom. The basal component in ECUT-111 is a paddlewheel unit, where two Co(II) ions are combined together by four carboxyl groups. Interestingly, different from the common encountered Co_2 paddlewheel unit that contains two terminal coordinated water molecules as potential open-metal sites,[6] the paddlewheel unit in ECUT-111 connects to two L^{2-} ligands through Co−N coordination bonds (Figure 1a). Thus, it affords 6-connectivity, rather than the common 4-connectivity. For each L^{2-} ligand, it binds to five Co(II) ions through two carboxyl groups in the bidentate mode and one imidazole unit.

In ECUT-111, there are two kinds of cages. Cage A (Figure 1b and Figure S2) is composed of 12 Co(II) ions and 6 L^{2-} ligands. The size of the inner aperture is about 5.2 Å; however, a narrow window of 4.0 Å permitting the entrance of a guest is observed. Cage B (Figure 1c and Figure S3) is made up of 24 Co(II) ions and 24 L^{2-} ligands, affording a large inner aperture of about 10.6 Å but also a narrow window of 4.0 Å. Figure 1d describes the 3D cage-based framework with 1D regular channels, where that cages A and B are in-turn connected together (Figure 1e).

The stability of ECUT-111 was initially explored by a thermogravimetric analysis (Figure S4), where the major loss before 260 °C is the loss of one C_2H_5OH molecule and one DMF molecule (experimental, 30.0%; calculated, 29.2%). Thereby, the chemical formula of ECUT-111 is Co(L)·DMF·C_2H_5OH. A platform was observed before 325 °C, indicative of high thermal stability. We further tested CH_3OH-exchanged samples, where the temperature of the loss of solvent molecules was decreased, and the first major loss was completed before 140 °C, showing the success of the solvent exchange between DMF and CH_3OH. In this regard, we set the activating temperature as 140 °C. Interestingly, the CH_3OH-exchanged samples render a platform with a high temperature up to 350 °C. The stability of the activated samples was confirmed by a PXRD study (Figure S5).

ECUT-111 affords a high N_2 uptake of up to 410 cm^3/g at 77 K and 1 bar. The adsorption isotherm presents a typical type I adsorption, indicative of the microporous framework of ECUT-111. A high BET specific surface area of up to 1493 m^2/g with a total pore volume of up to 0.63 cm^3/g was observed (Figure 2a). Two narrow pores with sizes of 5.8 and 9.1 Å were observed, comparable to the crystal data.

The high porosity and cage feature inspired us to further explore the SO_2 adsorption property. At 1 bar and 298 K, ECUT-111 enables an ultrahigh SO_2 uptake of up to 11.6 mmol/g (Figure 2b). This value exceeds those of most porous adsorbents composed of commercial porous carbon (3.3 mmol/g)[16c] and MOFs such as MFM-202a (10.2 mmol/g),[17] MFM-300(In) (8.28 mmol/g),[18,19] MFM-300(Sc) (9.4 mmol/g),[16a] NU-1000 (10.9 mmol/g),[16b] SIFSIX-1-Cu (11.01 mmol/g),[16k] and SIFSIX-2-Cu-i (6.9 mmol/g)[16k] and just below MFM-601 (12.3 mmol/g),[16j] MFM-170 (17.5 mmol/g),[16l] and MIL-101(Cr)-4F (18.4 mmol/g).[16a] Even at a low pressure of 0.1 bar, the SO_2 uptake in ECUT-111 is also outstanding, up to 6.4 mmol/g, comparable with that of one benchmark MOF, SIFSIX-2-Cu-i (6.01 mmol/g).[16k] For SO_2 removal such as flue gas desulfurization, it requires not only a large SO_2 uptake at low pressure but also SO_2 selectivity over CO_2 and N_2. Thus, we further carried out both CO_2 and N_2 adsorption tests (Figure 2b). The adsorption capacity at 298 K and 1 bar is 3.3 mmol/g for CO_2 and 0.18 mmol/g for N_2, far smaller than that for SO_2, indicative of the selective adsorption of SO_2 over CO_2 and N_2. A similar trend is also observed at low pressure (0.1 bar), 0.54 mmol/g for CO_2 and 0.02 mmol/g for N_2; the corresponding SO_2 value is almost 12-fold and 320-fold of those for CO_2 and N_2.

To estimate the magnitude of the selectivity toward SO_2, we first carried out the calculation for the Henry constant and the Henry selectivity on the basis of the adsorption data at low pressure. The Henry constants are 56.6 mmol/(g bar) for SO_2 (Figure S6), 4.6 mmol/(g bar) for CO_2 (Figure S7), and 0.18 mmol/(g bar) for N_2 (Figure S8), respectively, giving the corresponding Henry selectivities of 12 for SO_2/CO_2 and 314 for SO_2/N_2. Furthermore, we carried out ideal adsorbed solution theory (IAST) calculations. The IAST selectivity is 22.2−25.2 for a 1/99 v/v SO_2/CO_2 mixture and 596.9−860.9 for a 1/99 v/v SO_2/N_2 mixture (Figure 2c). The results suggest highly selective adsorption of SO_2 over CO_2 and N_2 and consequently the potential application of ECUT-11 in SO_2 removal.

The affinity between the MOF skeleton and guest molecules was investigated and was reflected by the Q_{st} value. Then, SO_2, CO_2, and N_2 adsorption at 273 K was tested, and the Q_{st} values (Figure S9) were deduced to be 33.2 kJ/mol for SO_2, 29.6 kJ/mol for CO_2, and 9.9 kJ/mol for N_2, strongly suggesting different affinities among these guest molecules in the sequence SO_2 > CO_2 > N_2, quite consistent with the adsorption results.

To obtain the real separation, we further carried out an experimental breakthrough test. A ECUT-111-filled column (0.5 g) was made and used for a breakthrough test. As shown in Figure 2d, complete separation of SO_2 from a SO_2/CO_2 mixture containing 2000 ppm of SO_2 was observed, where CO_2 breaks from the column after 28 min/g, whereas an outflow of SO_2 is detected after 187 min/g, providing a long separation time of 159 min/g. This breakthrough experiment was then repeated three times without any decrease in the separation time (Figure 2e), suggesting excellent recycle use. For a $SO_2/CO_2/N_2$ mixture containing 1000 ppm of SO_2, an ECUT-111-filled column is also effective, as evidenced by the breakthrough time of 6 min/g for N_2, 12 min/g for CO_2, and 98 min/g for SO_2 (Figure 2f). Excellent recycle use was also observed for this $SO_2/CO_2/N_2$ mixture (Figure S10). As we know, the difficulty for SO_2 removal upon MOF adsorbents is the validity under humid conditions. Impressively, our MOF under humid conditions (3% water) shows separation performance comparable to that under dry conditions (Figure 2f). The stability of the material after a breakthrough test was also supported by a PXRD study (Figure S11). All of the above results suggest our MOF has a superior ability for applications in SO_2 removal.

Furthermore, in order to expain the adsorption mechanism, a DFT calculation was carried out. The binding energy of SO_2 with the MOF framework is −0.05 eV, suggesting that the thermokinetics of SO_2 adsorption is favorable, whereas for

https://dx.doi.org/10.1021/acs.inorgchem.1c00033
Inorg. Chem. 2021, 60, 3447−3451

CO_2 the binding energy is 0.56 eV, implying undesired thermokinetical adsorption; this strongly suggests the selective adsorption of SO_2 over CO_2.

CONCLUSION

In conclusion, we have demonstrated herein the synthesis, structure, porosity, and separation properties of a new cage-based MOF. The new MOF contains two distinct cages with microporous features but a narrow window size. This permits the MOF to render both high SO_2 uptake and high SO_2/CO_2 selectivity, thus leading to complete separation of SO_2 from SO_2/CO_2 and $SO_2/CO_2/N_2$ mixtures just containing ppm level SO_2. The excellent chemical stability further gives this MOF good recycle ability and application even under humid conditions, meeting the practical demand for flue gas desulfurization or other SO_2-containing desulfurizations. The results also outline that cage-based MOFs would be good candidates for separation, as this class often contains large inherent inner pores but a narrow window, thus creating a good tradeoff between adsorption capacity and selectivity. Moreover, as shown in this MOF, although it shows high SO_2 adsorption capacity, the SO_2/CO_2 selectivity is just moderate; this is mainly because of the larger window size, relative to the size of SO_2. Therefore, there still a need for further design to construct cage-based MOFs with a narrow window close to the size of SO_2 but a large aperture, thus affording both large SO_2 adsorption capacity and high SO_2/CO_2 selectivity.

ASSOCIATED CONTENT

Supporting Information

The Supporting Information is available free of charge at https://pubs.acs.org/doi/10.1021/acs.inorgchem.1c00033.

Details of the syntheses and additional figures as described in the text (PDF)

Accession Codes

CCDC 2047694 contains the supplementary crystallographic data for this paper. These data can be obtained free of charge via www.ccdc.cam.ac.uk/data_request/cif, or by emailing data_request@ccdc.cam.ac.uk, or by contacting The Cambridge Crystallographic Data Centre, 12 Union Road, Cambridge CB2 1EZ, UK; fax: +44 1223 336033.

AUTHOR INFORMATION

Corresponding Author

Feng Luo − *School of Biology, Chemistry and Material Science, East China University of Technology, Nanchang, Jiangxi 344000, People's Republic of China;* orcid.org/0000-0001-6380-2754; Email: ecitluofeng@163.com

Authors

Meng Jia Yin − *School of Biology, Chemistry and Material Science, East China University of Technology, Nanchang, Jiangxi 344000, People's Republic of China*

Xiao Hong Xiong − *School of Biology, Chemistry and Material Science, East China University of Technology, Nanchang, Jiangxi 344000, People's Republic of China*

Xue Feng Feng − *School of Biology, Chemistry and Material Science, East China University of Technology, Nanchang, Jiangxi 344000, People's Republic of China*

Wen Yuan Xu − *College of Chemistry and Chemical Engineering, Hunan Institute of Science and Technology, Yueyang 414006, China*

Rajamani Krishna − *Van't Hoff Institute for Molecular Sciences, University of Amsterdam, 1098 XH Amsterdam, The Netherlands;* orcid.org/0000-0002-4784-8530

Complete contact information is available at: https://pubs.acs.org/10.1021/acs.inorgchem.1c00033

Author Contributions

The manuscript was written through contributions of all authors.

Notes

The authors declare no competing financial interest.

ACKNOWLEDGMENTS

We thank the National Science Foundations of China (21966002, 21871047, and 21761001), the Natural Science Foundation of Jiangxi Province of China (20181ACB20003), and the Training Program for Academic and Technical Leaders of Major Disciplines in Jiangxi Province (20194BCJ22010).

REFERENCES

(1) (a) Kalaj, M.; Bentz, K. C.; Ayala, S., Jr.; Palomba, J. M.; Barcus, K. S.; Katayama, Y.; Cohen, S. M. MOF-polymer hybrid materials: from simple composites to tailored architectures. *Chem. Rev.* **2020**, *120*, 8267−8302. (b) Bai, Y.; Dou, Y. B.; Xie, L. H.; Rutledge, W.; Li, J. R.; Zhou, H. C. Zr-based metal-organic frameworks: design, synthesis, structure, and applications. *Chem. Soc. Rev.* **2016**, *45*, 2327−2367. (c) Zhang, H. P.; Fan, Y. L.; Krishna, R.; Feng, X. F.; Wang, L.; Luo, F. Robust metal-organic framework with multiple traps for trace Xe/Kr separation. *Sci. Bull.* **2020**, DOI: 10.1016/j.scib.2020.12.031. (d) Fan, Y. L.; Zhang, H. P.; Yin, M. J.; Krishna, R.; Feng, X. F.; Wang, L.; Luo, M. B.; Luo, F. High adsorption capacity and selectivity of SO_2 over CO_2 in a metal-organic framework. *Inorg. Chem.* **2021**, *60*, 4−8.

(2) Stock, N.; Biswas, S. Synthesis of metal-organic frameworks (MOFs): routes to various MOF topologies, morphologies, and composites. *Chem. Rev.* **2012**, *112*, 933−969.

(3) Rice, A. M.; Martin, C. R.; Galitskiy, V. A.; Berseneva, A. A.; Leith, G. A.; Shustova, N. B. Photophysics modulation in photoswitchable metal-organic frameworks. *Chem. Rev.* **2020**, *120*, 8790−8813.

(4) Chen, Z. J.; Jiang, H.; Li, M.; O'Keeffe, M.; Eddaoudi, M. Reticular chemistry 3.2: typical minimal edge-transitive derived and related nets for the design and synthesis of metal-organic frameworks. *Chem. Rev.* **2020**, *120*, 8039−8065.

(5) Feng, L.; Wang, K. Y.; Lv, X. L.; Yan, T. H.; Li, J. R.; Zhou, H. C. Modular total synthesis in reticular chemistry. *J. Am. Chem. Soc.* **2020**, *142*, 3069−3076.

(6) Li, H. L.; Eddaoudi, M.; Groy, T. L.; Yaghi, O. M. Establishing microporosity in open metal-organic frameworks: gas sorption isotherms for Zn(BDC)(BDC = 1,4-benzenedicarboxylate). *J. Am. Chem. Soc.* **1998**, *120*, 8571−8572.

(7) Zhai, Q. G.; Bu, X. H.; Zhao, X.; Li, D. S.; Feng, P. Y. Pore space partition in metal-organic frameworks. *Acc. Chem. Res.* **2017**, *50*, 407−417.

(8) Ma, J. X.; Xu, N.; Liu, Y.; Wang, Y.; Li, H.; Liu, G. C.; Wang, X. L.; Li, J. R. A stable 3D Zn-coordination polymer sensor based on dual luminescent ligands for efficient detection of multiple analytes under acid or alkaline environment. *Inorg. Chem.* **2020**, *59*, 15495−15503.

(9) Xu, Z. Z.; Xiong, X. H.; Xiong, J. B.; Krishna, R.; Li, L. B.; Fan, Y. L.; Luo, F.; Chen, B. L. A robust Th-azole framework for highly efficient purification of C_2H_4 from a $C_2H_4/C_2H_2/C_2H_6$ mixture. *Nat. Commun.* **2020**, *11*, 3163.

(10) Schoedel, A.; Li, M.; Li, D.; O'Keeffe, M.; Yaghi, O. M. Structures of metal-organic frameworks with rod secondary building units. *Chem. Rev.* **2016**, *116*, 12466−12535.

(11) (a) Cui, X. L.; Chen, K. J.; Xing, H. B.; Yang, Q. W.; Krishna, R.; Bao, Z. B.; Wu, H.; Zhou, W.; Dong, X. L.; Han, Y.; Li, B.; Ren, Q. L.; Zaworotko, M. J.; Chen, B. L. Pore chemistry and size control in hybrid porous materials for acetylene capture from ethylene. *Science* **2016**, *353*, 141−144. (b) Peng, Y. L.; Pham, T.; Li, P. F.; Wang, T.; Chen, Y.; Chen, K. J.; Forrest, K. A.; Space, B.; Cheng, P.; Zaworotko, M. J.; Zhang, Z. J. Robust ultramicroporous metal-organic frameworks with benchmark affinity for acetylene. *Angew. Chem., Int. Ed.* **2018**, *57*, 10971−10975. (c) Luo, F.; Yan, C. S.; Dang, L. L.; Krishna, R.; Zhou, W.; Wu, H.; Dong, X. L.; Han, Y.; Hu, T. L.; O'Keeffe, M.; Wang, L. L.; Luo, M. B.; Lin, R. B.; Chen, B. L. UTSA-74: a MOF-74 isomer with two accessible binding sites per metal center for highly selective gas separation. *J. Am. Chem. Soc.* **2016**, *138*, 5678−5684. (d) Shi, Z. L.; Tao, Y.; Wu, J. S.; Zhang, C. Z.; He, H. L.; Long, L. L.; Lee, Y. J.; Li, T.; Zhang, Y. B. Robust metal-triazolate frameworks for CO_2 capture from flue gas. *J. Am. Chem. Soc.* **2020**, *142*, 2750−2754.

(12) (a) Chen, L.; Chen, Q. H.; Wu, M. Y.; Jiang, F. L.; Hong, M. C. Controllable coordination-driven self-assembly: from discrete metal-locages to infinite cage-based frameworks. *Acc. Chem. Res.* **2015**, *48*, 201−210. (b) He, Y. P.; Chen, G. H.; Yuan, L. B.; Zhang, L.; Zhang, J. Ti_4(embonate)$_6$ cage-ligand strategy on the construction of metal-organic frameworks with high stability and gas sorption properties. *Inorg. Chem.* **2020**, *59*, 964−967. (c) Liu, B.; Wu, W. P.; Hou, L.; Li, Z. S.; Wang, Y. Y. Two nanocage-based metal-organic frameworks with mixed-cluster SBUs and CO_2 sorption selectivity. *Inorg. Chem.* **2015**, *54*, 8937−8942.

(13) (a) Laurent, A.; Espinosa, N. Environmental impacts of electricity generation at global, regional and national scales in 1980−2011: what can we learn for future energy planning? *Energy Environ. Sci.* **2015**, *8*, 689−701. (b) Fioletov, V. E.; McLinden, C. A.; Krotkov, N.; Li, C.; Joiner, J.; Theys, N.; Carn, S.; Moran, M. D. A Global catalogue of large SO_2 sources and emissions derived from the ozone monitoring instrument. *Atmos. Chem. Phys.* **2016**, *16*, 11497−11519.

(14) (a) United States Environmental Protection Agency. *Sulfur oxides control technology series: flue gas desulfurization magnesium oxide process, summary report No. 4/1981* (EPA, 1981). (b) Mathieu, Y.; Tzanis, L.; Soulard, M.; Patarin, J.; Vierling, M.; Molière, M. Adsorption of SO_x by oxide materials: a review. *Fuel Process. Technol.* **2013**, *114*, 81−100.

(15) (a) Han, X.; Yang, S.; Schroder, M. Porous metal-organic frameworks as emerging sorbents for clean air. *Nat. Rev. Chem.* **2019**, *3*, 108−118. (b) Grape, E. S.; Flores, J. G.; Hidalgo, T.; Martínez-Ahumada, E.; Gutiérrez-Alejandre, A.; Hautier, A.; Williams, D. R.; O'Keeffe, M.; Öhrström, L.; Willhammar, T.; Horcajada, P.; Ibarra, I. A.; Inge, A. K. A robust and biocompatible bismuth ellagate MOF synthesized under green ambient conditions. *J. Am. Chem. Soc.* **2020**, *142*, 16795−16804. (c) Guo, L. J.; Feng, X. F.; Gao, Z.; Krishna, R.; Luo, F. Robust 4d-5f bimetal-organic framework for efficient removal of trace SO_2 from SO_2/CO_2 and $SO_2/CO_2/N_2$ mixture. *Inorg. Chem.* **2021**, *60*, 1310. (d) Fan, Y. L.; Yin, M. J.; Krishna, R.; Feng, X. F.; Luo, F. Constructing robust gigantic drum-like hydrophobic [$Co_{24}U_6$] nanocage in metal-organic framework for high-performance SO_2 removal at humidity condition. *J. Mater. Chem. A* **2021**, DOI: 10.1039/D0TA10004H.

(16) (a) Martinez-Ahumada, E.; Diaz-Ramirez, M. L.; Lara-Garcia, H. A.; Williams, D. R.; Martis, V.; Jancik, V.; Lima, E.; Ibarra, I. A. High and reversible SO_2 capture by a chemically stable Cr(III)-based MOF. *J. Mater. Chem. A* **2020**, *8*, 11515−11520. (b) Gorla, S.; Díaz-Ramírez, M. L.; Abeynayake, N. S.; Kaphan, D. M.; Williams, D. R.; Martis, V.; Lara-García, H. A.; Donnadieu, B.; Lopez, N.; Ibarra, I. A.; Montiel-Palma, V. Functionalized NU-1000 with an iridium organo-metallic fragment: SO_2 capture enhancement. *ACS Appl. Mater. Interfaces* **2020**, *12*, 41758−41764. (c) Zárate, J. A.; Sánchez-González, E.; Williams, D. R.; González-Zamora, E.; Martis, V.; Martínez, A.; Balmaseda, J.; Maurin, G.; Ibarra, I. A. High and energy-efficient reversible SO_2 uptake by a robust Sc(III)-based MOF. *J. Mater. Chem. A* **2019**, *7*, 15580−15584. (d) Mukherjee, S.; Sensharma, D.; Chen, K. J.; Zaworotko, M. J. Crystal engineering of porous coordination networks to enable separation of C_2 hydrocarbons. *Chem. Commun.* **2020**, *56*, 10419−10441. (e) Liang, J.; Xing, S.; Brandt, P.; Nuhnen, A.; Schlusener, C.; Sun, Y.; Janiak, C. A chemically stable cucurbit uril-based hydrogen-bonded organic framework for potential SO_2/CO_2 separation. *J. Mater. Chem. A* **2020**, *8*, 19799−19804. (f) Britt, D.; Tranchemontagne, D.; Yaghi, O. M. & Yaghi, O. M. Metal-organic frameworks with high capacity and selectivity for harmful gases. *Proc. Natl. Acad. Sci. U. S. A.* **2008**, *105*, 11623−11627. (g) Thallapally, P. K.; Motkuri, R. K.; Fernandez, C. A.; McGrail, B. P.; Behrooz, G. S. & Behrooz, G. S. Prussian blue analogues for CO_2 and SO_2 capture and separation applications. *Inorg. Chem.* **2010**, *49*, 4909−4915. (h) Tan, K.; Canepa, P.; Gong, Q.; Liu, J.; Johnson, D. H.; Dyevoich, A.; Thallapally, P. K.; Thonhauser, T.; Li, J.; Chabal, Y. J. Mechanism of preferential adsorption of SO_2 into two microporous paddle wheel frameworks M(bdc)(ted)$_{0.5}$. *Chem. Mater.* **2013**, *25*, 4653−4662. (i) Savage, M.; Cheng, Y. Q.; Easun, Ti. L.; Eyley, J. E.; Argent, S. P.; Warren, M. R.; Lewis, W.; Murray, C.; Tang, C. C.; Frogley, M. D.; Cinque, G.; Sun, J. L.; Rudi, S.; Murden, R. T.; Benham, M. J.; Fitch, A. N.; Blake, A. J.; Ramirez-Cuesta, A. J.; Yang, S. H.; Schrder, M. Selective adsorption of sulfur dioxide in a robust metal-organic framework material. *Adv. Mater.* **2016**, *28*, 8705−8711. (j) Carter, J. H.; Han, X.; Moreau, F. Y.; da Silva, I.; Nevin, A.; Godfrey, H. G. W.; Tang, C. C.; Yang, S. H.; Schröder, M. Exceptional adsorption and binding of sulfer dioxide in a robust zirconium-based metal-organic framework. *J. Am. Chem. Soc.* **2018**, *140*, 15564−15567. (k) Cui, X.; Yang, Q. W.; Yang, L. F.; Krishna, R.; Zhang, Z. G.; Bao, Z. B.; Wu, H.; Ren, Q. L.; Zhou, W.; Chen, B. L.; Xing, H. B. Ultrahigh and selective SO_2 uptake in inorganic anion-pillared hybrid porous materials. *Adv. Mater.* **2017**, *29*, 1606929. (l) Smith, G. L.; Eyley, J. E.; Han, X.; Zhang, X.; Li, J.; Jacques, N. M.; Godfrey, H. G. W.; Argent, S. P.; McCormick McPherson, L. J.; Teat, S. J.; Cheng, Y.; Frogley, M. D.; Cinque, G.; Day, S. J.; Tang, C. C.; Easun, T. L.; Rudic, S.; Ramirez-Cuesta, A. J.; Yang, S.; Schroder, M. Reversible coordinative binding and separation of sulfur dioxide in a robust metal-organic framework with open copper sites. *Nat. Mater.* **2019**, *18*, 1358−1365.

(17) Yang, S.; Liu, L.; Sun, J.; Thomas, K. M.; Davies, A. J.; George, M. W.; Blake, A. J.; Hill, A. H.; Fitch, A. N.; Tang, C. C.; Schroder, M. Irreversible network transformation in a dynamic porous host catalyzed by sulfur dioxide. *J. Am. Chem. Soc.* **2013**, *135*, 4954−4957.

(18) Savage, M.; Cheng, Y.; Easun, T. L.; Eyley, J. E.; Argent, S. P.; Warren, M. R.; Lewis, W.; Murray, C.; Tang, C. C.; Frogley, M. D.; Cinque, G.; Sun, J.; Rudić, S.; Murden, R. T.; Benham, M. J.; Fitch, A. N.; Blake, A. J.; Ramirez-Cuesta, A. J.; Yang, S.; Schroder, M. Selective adsorption of sulfur dioxide in a robust metalorganic framework material. *Adv. Mater.* **2016**, *28*, 8705−8711.

(19) Yang, S.; Sun, J.; Ramirez-Cuesta, A. J.; Callear, S. K.; David, W. I. F. D. P.; Newby Anderson, R.; Blake, A. J.; Parker, J. E.; Tang, C. C.; Schroder, M. Selectivity and direct visualization of carbon dioxide and sulfur dioxide in a decorated porous host. *Nat. Chem.* **2012**, *4*, 887−894.

https://dx.doi.org/10.1021/acs.inorgchem.1c00033
Inorg. Chem. 2021, 60, 3447−3451

A Robust Cage-Based Metal-Organic Framework Showing Ultrahigh SO_2 Uptake for Efficient Removal of Trace SO_2 from SO_2/CO_2 and $SO_2/CO_2/N_2$ Mixture

Meng Jia Yin,[a] Xiao Hong Xiong,[a] Xue Feng Feng,[a] Wen Yuan Xu,[c] Rajamani Krishna,[c] and Feng Luo[a]*

[a]School of Biology, Chemistry and Material Science, East China University of Technology, Nanchang, Jiangxi 344000, China

[b]College of Chemistry and Chemical Engineering, Hunan Institute of Science and Technology, Yueyang 414006, China

[c]Van't Hoff Institute for Molecular Sciences, University of Amsterdam, Science Park 904, 1098 XH Amsterdam, The Netherlands

Corresponding author: Feng Luo, ecitluofeng@163.com

Experimental Methods

Materials and Physical Measurements. All chemicals are directly purchased from innochem with no further purification. The data of X-ray powder diffraction were collected on a Bruker AXSD8 Discover powder diffractometer at 40 kV/40 mA for Cu Kα (λ = 1.5406 Å) at room temperature in the range of 5-50 °(2θ) with a scan speed of 0.1 °per step. Thermogravimetric analysis (TG) was performed by a TGA Q500 thermal analysis system. All TGA experiments were performed under a N_2 atmosphere from 40-800°C at a rate of 5°C /min. The gas sorption isotherms were collected on ASAP2020 PLUS (anti-corrosion version). Ultrahigh-purity-grade (>99.999%) N_2, CO_2, and SO_2 gases were used in this adsorption measurement. To maintain the experimental temperatures liquid nitrogen (77 K) and temperature-programmed water bath (273 and 298 K) were used respectively.

Synthesis of ECUT-111. 5-(1H-imidazol-1-yl) isophthalic acid (15 mg)，$Co(NO_3)_2 \cdot 6H_2O$ (10 mg) in a mixed solution of DMF (4mL) and C_2H_5OH (1mL) with 200 μL HNO_3. The reaction temperature and time is 150℃ and three day. Pure red block crystals were obtained with yield up to 75% based on Co. Element analysis (%) is calc. C/47.07, H/4.69, N/10.29; exp. C/47.12, H/4.66, N/10.35.

Degassing ECUT-111. 100 mg MOF crystals were soaked in methanol for three days and fresh methanol was added every 8 h. After decanting the methanol extract, the sample was dried at room temperature overnight, then further degassed using ASAP2020 PLUS for 24 h at 140°C.

X-ray Crystallography. X-ray diffraction data of **ECUT-100** were collected at room temperature on a Bruker Appex II CCD diffractometer using graphite monochromated MoKα radiation (λ=0.71073 Å). The data reduction included a correction for Lorentz and polarization effects, with an applied multi-scan absorption correction (SADABS). The crystal structure was solved and refined using the SHELXTL program suite. Direct methods yielded all non-hydrogen atoms, which were refined with anisotropic thermal parameters. All hydrogen atom positions were calculated geometrically and were riding on their respective atoms. The SQUEEZE subroutine of the PLATON software suite was used to remove the scattering from the highly disordered guest molecules. CCDC 2047694 contains the supplementary crystallographic data of **ECUT-111**. These data can be obtained free of charge from the Cambridge Crystallographic Data Centre via www.ccdc.cam.ac.uk/data_request/cif.

Calculation method. The density functional theory (DFT) calculations were performed by using the Vienna Ab initio Simulation Package (VASP) code with the projector augmented wave (PAW) method.[1-2] The exchange-functional was treated using the generalized gradient approximation (GGA) of Perdew-Burke-Ernzerhof (PBE) functional.[3] The Hubbard *U* (DFT+*U*) corrections of transition metal (3.42 for Cobalt) was considered in the calculations.[4] Wave functions were expanded using a

plane-wave basis set with kinetic energy cutoff of 500 eV and the geometries were fully relaxed until the residual force convergence value on each atom being less 0.05 eV/Å. The Brillouin zone integration was performed using 2×2×2 Monkhorst-Pack k-point sampling for structural optimization and energy calculation.[5] The self-consistent calculations applied a convergence energy threshold of 10^{-4} eV. Spin-polarization was considered in all calculations.

The elementary reaction could be defined as the CO_2/SO_2 molecules were physic adsorbed in the cage by imidazole ligand *via* C-H···O interactions:

$$\mathrm{MOF} + \ 6(\mathrm{CO_2/SO_2}) \rightarrow \mathrm{MOF} - \frac{\mathrm{CO_2}}{\mathrm{MOF}} - \mathrm{SO_2}$$

The formula of average adsorption energy was defined:

$$\Delta \mathrm{G}_b = [E(\mathrm{MOF} - \mathrm{CO_2/MOF} - \mathrm{SO_2}) - E(\mathrm{MOF}) - E(\mathrm{CO_2/SO_2}) \ * 18]/18$$

Fitting of experimental data on pure component isotherms

The isotherm data for SO_2, CO_2, and N_2 in ECUT-111 at 273 K, and 298 K were fitted with very good accuracy using the 1-site Langmuir model

$$q = \frac{q_{sat} bp}{1 + bp}$$

with *T*-dependent parameter *b*

$$b = b_0 \exp\left(\frac{E}{RT}\right)$$

The unary isotherm fit parameters for SO_2, CO_2, and N_2 are provided in Table S1.

Table S1. 1-site Langmuir parameter fits for SO_2, CO_2, and N_2 in ECUT-111.

	q_{sat} mol kg^{-1}	b_0 Pa^{-1}	E kJ mol^{-1}
SO_2	13	1.367E-10	33.2
CO_2	8	4.269E-11	29.6
N_2	1.6	2.259E-08	9.9

Isosteric heat of adsorption

The binding energy is reflected in the isosteric heat of adsorption, Q_{st}, is calculated from the Clausi us-Clapeyron equation.

$$Q_{st} = -RT^2 \left(\frac{\partial \ln p}{\partial T} \right)_q \quad \square\square\square$$

IAST calculations of adsorption selectivities and uptake capacities

We consider the separation of binary 1/99 SO_2/CO_2 mixtures and 1/99 SO_2/N_2 mixtures at 298 K. The adsorption selectivity for SO_2/CO_2 and SO_2/N_2 separation is defined by

$$S_{ads} = \frac{q_1/q_2}{p_1/p_2}$$

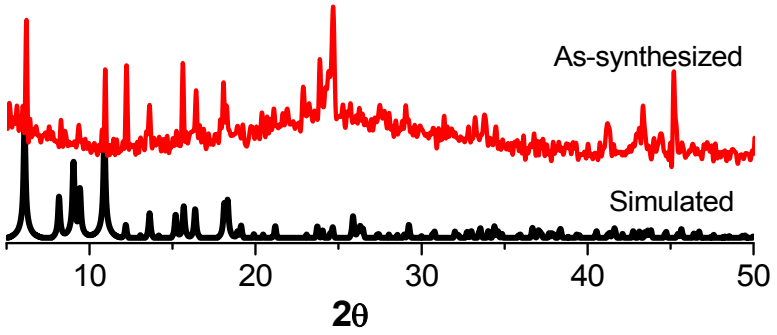

Figure S1. A comparison of PXRD patterns of the simulated data and the as-synthesized samples.

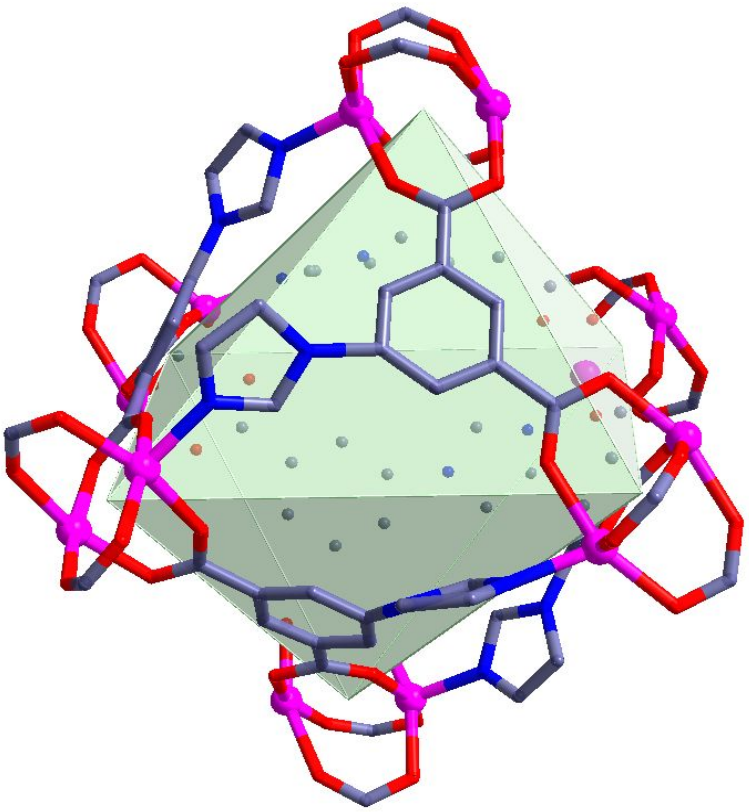

Figure S2. View of the octahedral geometry of cage A.

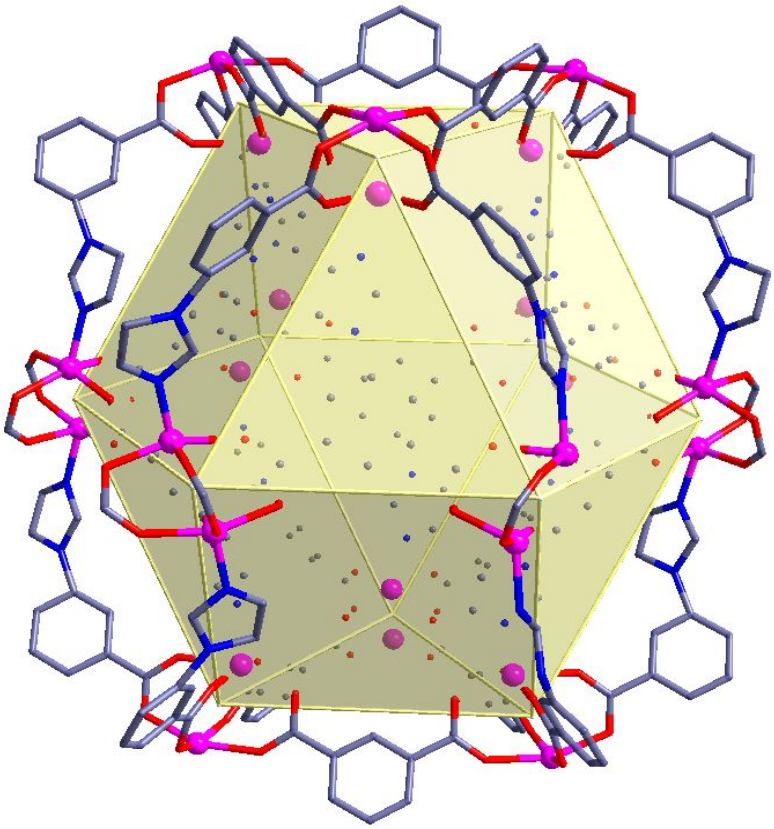

Figure S3. View of the polyhedron geometry of cage B.

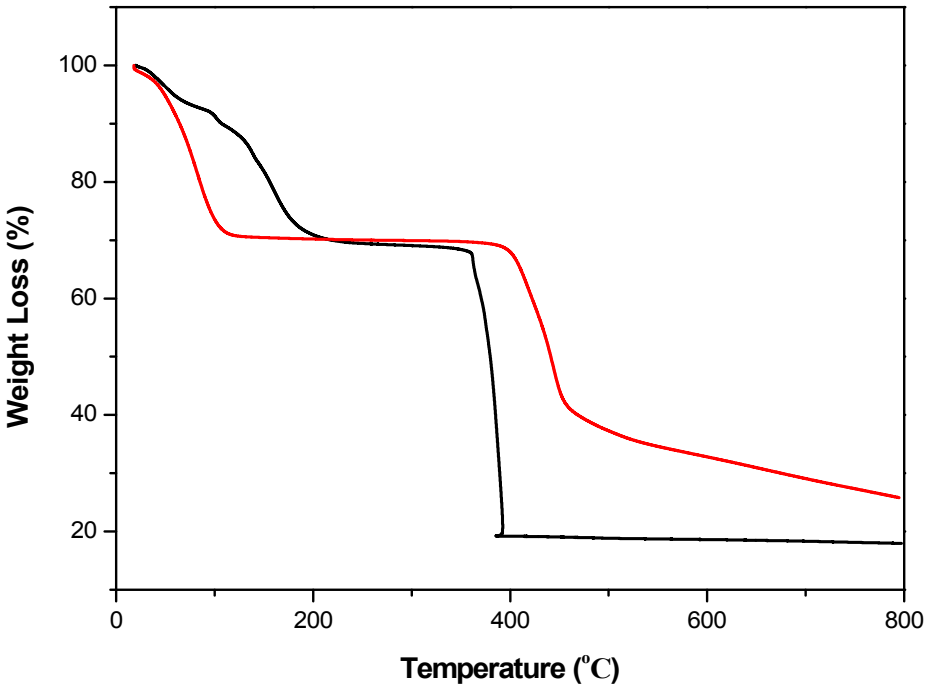

Figure S4. The TG polts of **ECUT-111** (black) and the CH_3OH-exchanged samples (red).

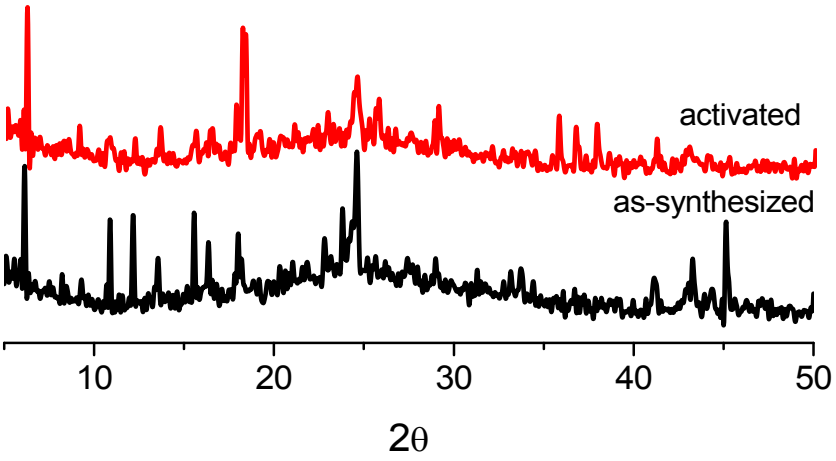

Figure S5. A comparison of PXRD patterns for the as-synthesized samples and the activated samples.

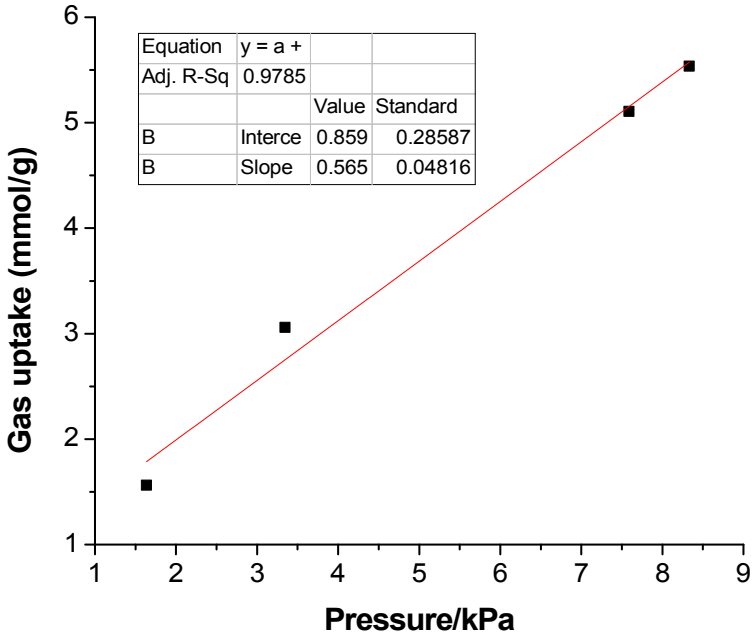

Figure S6. The Henry fitting of SO_2 adsorption on ECUT-111.

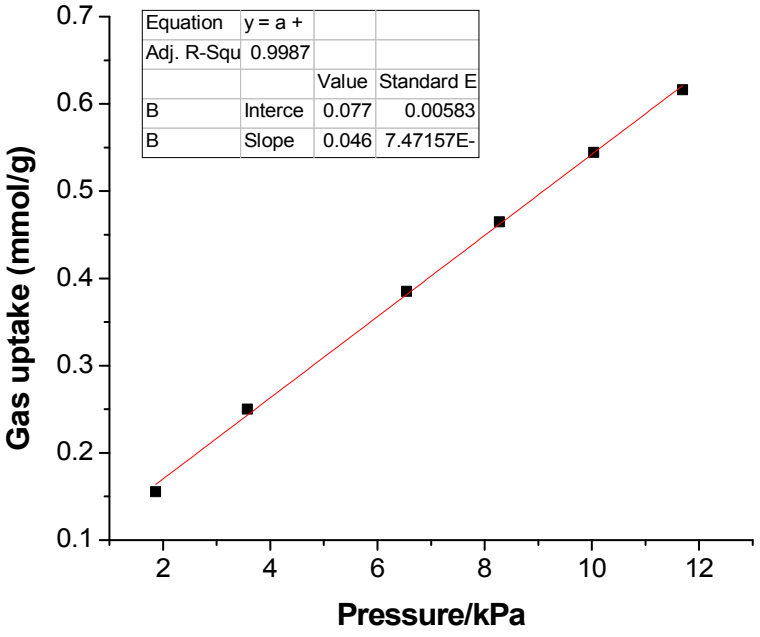

Figure S7. The Henry fitting of CO_2 adsorption on ECUT-111.

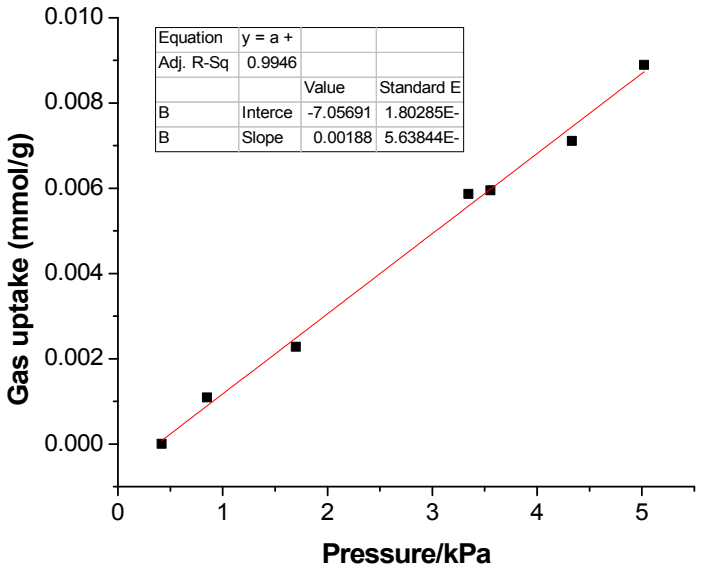

Figure S8. The Henry fitting of N_2 adsorption on ECUT-111.

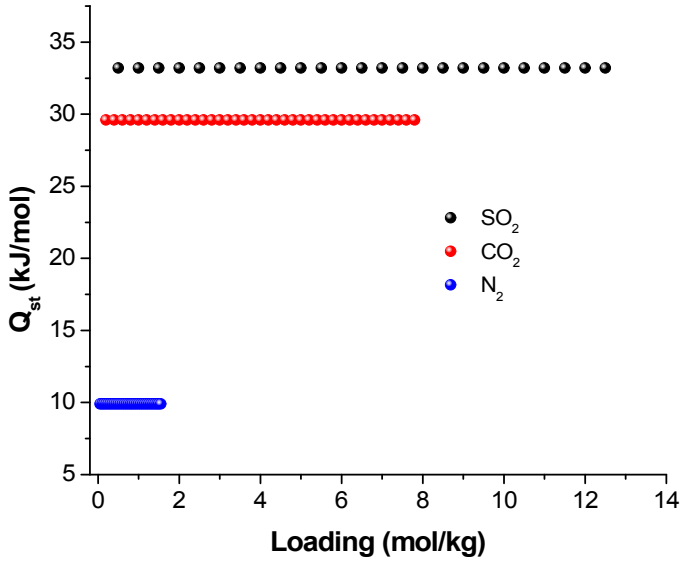

Figure S9. The Q_{st} of SO_2, CO_2, and N_2.

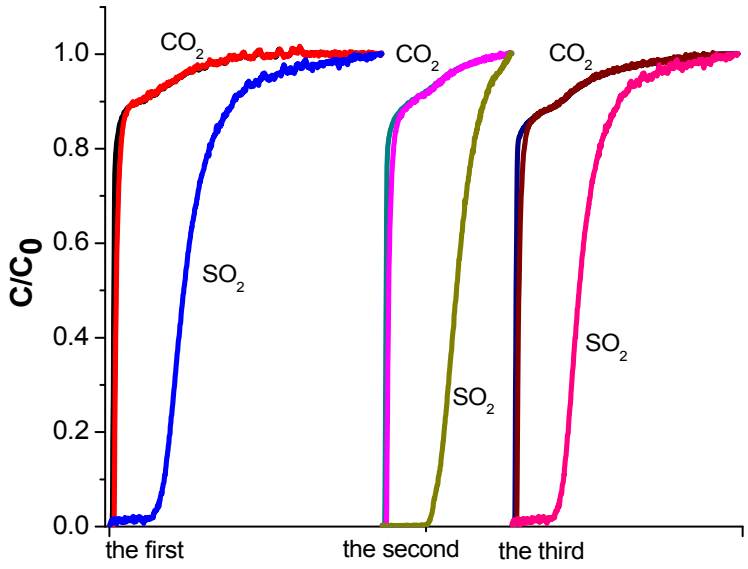

Figure S10. The recycle use of breakthrough test for $SO_2/CO_2/N_2$ mixture.

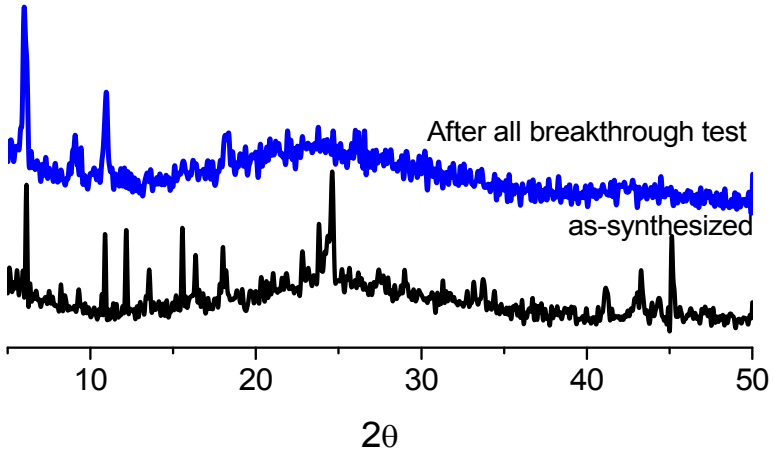

Figure S11. A comparison of PXRD patterns for the as-synthesized samples and the samples after all breakthrough test.

[1] Perdew, J. P.; Burke, K.; Ernzerhof, M. Generalized gradient approximation made simple. Physical review letters 1996, 77, 3865.

[2] Kresse, G.; Joubert, D. From ultrasoft pseudopotentials to the projector augmented-wave method. Physical Review B 1999, 59, 1758.

[3] Kim, H.; Lee, K.; Woo, S. I.; Jung, Y. On the mechanism of enhanced oxygen reduction reaction in nitrogen-doped graphene nanoribbons. *Physical Chemistry Chemical Physics* ***2011,*** *13*, 17505-17510.

[4] Gong, L.; Wang X.; Zheng T.; Liu J.; Wang J.; Yang Y.-C.; Zhang J.; Han X.; Zhang L.; Xia Z. Catalytic Mechanism and Design Principle of Coordinately Unsaturated Single Metal Atom-Doped Covalent Triazine Frameworks with High Activity and Selectivity for CO_2 Electroreduction. doi.org/10.1039/D0TA10875H.

[5] Chadi, D. Special points for Brillouin-zone integrations. Physical Review B 1977, 16, 1746.